Applied Physics Letters ARTICLE scitation.org/journal/apl

Using irradiation-induced defects as pinning sites to minimize self-alignment in twisted bilayer graphene

Cite as: Appl. Phys. Lett. **118**, 151602 (2021); doi: 10.1063/5.0039703
Submitted: 5 December 2020 · Accepted: 22 March 2021 ·
Published Online: 16 April 2021

Di Chen[1,2] and Lin Shao[3,a)]

AFFILIATIONS

[1]The Texas Center for Superconductivity, University of Houston, Houston, Texas 77204, USA
[2]Department of Physics, University of Houston, Houston, Texas 77204, USA
[3]Department of Nuclear Engineering, Texas A&M University, College Station, Texas 77843, USA

[a)]**Author to whom correspondence should be addressed:** lshao@tamu.edu. **Tel.:** 9798454107

ABSTRACT

Preparing bi-layer graphene under a magic twisting angle of ∼1.1° has been challenging due to its strong tendency for self-alignment. We propose a method to pin graphene layers and minimize their self-rotation when positioned close to each other. The feasibility is demonstrated by the present study using molecular dynamics simulations. C_{60} clusters are used to bombard two individual graphene layers, creating damage on both layers. When two irradiated layers are moving closer to each other, defects from irradiation damaged zones can interact with each other, hence acting as pinning sites to immobilize graphene and minimize rotation or gliding. Dangling bonds from defective regions of each plane induce the formation of sp bonds. Upon sliding, the bond is strong enough to induce the formation of one-dimensional carbon single chain, acting as a thread to constrain the relative movements.

Two layers of graphene exhibit tunable electronic properties, from conductor to insulator, as a function of twisting angles.[1,2] The Dirac cones of the two layers shift and intersect, leading to hybridization and new flatband formation.[1,2] At a "magic" twisting angle of ∼1.1°, the system exhibits Mott insulator-like property and superconductivity.[1,2] These findings have stimulated intense research interest and opened new doors for graphene-based devices. The key is to control the graphene misalignment angle precisely. However, it was also reported in numerous studies that precise control of misalignment angles is very challenging. When one graphene layer is released to bond with another graphene layer under a specific misalignment angle, the interlayer interactions tend to realign both layers when they are close to each other.[3] Hence, the misalignment control is completely lost. Any slight heat or strain can induce re-alignment of graphene layers. A few research groups solved the problem by creating many twisted systems randomly and obtained the expected twisting based on luck.[3]

It is in great demand to develop a method that can be used to create twisted bi-layer systems at an arbitrary angle routinely. Here, we reported a method to immobilize graphene rotation by using irradiation-induced defects as pinning sites. The key step is to bombard graphene layers with ions or cluster ions to create defects prior to "bonding." When two layers are brought closer, these defective zones may induce C re-bonding, which serves as pinning to forbid graphene rotations. Since ion irradiation has been a mature industry processing, the method is feasible and highly repeatable. For the demonstration here, we used C_{60} molecules as projectiles due to the following reasons: (1) C_{60} molecule is a cage-like tightly packed carbon system which has superior stability and mechanical strength. Using C_{60} molecules as projectiles can create nanopore on graphene, with the pore size larger than the molecule size, which is about 0.7 nm. Such collision is guaranteed for each bombardment. (2) Using C_{60} molecule avoids potential doping and contamination problems on the graphene. (3) C_{60} cluster effusion source is commercially available.

In the present study, molecular dynamics (MD) simulations were performed using the large-scale atomic/molecular massively parallel simulator (LAMMPS) code.[4] The adaptive intermolecular reactive bond order (AIREBO) potential was used to describe carbon interactions.[5] This potential was selected due to its good prediction and agreement with experimental observation.[5] For example, the potential creates an interplanar spacing of 3.4 Å in graphite, which agrees with experimental results.[6] The Tersoff potential was smoothly linked to the Ziegler–Biersack–Littmark (ZBL) potential at a short interaction distance to simulate nuclei-nuclei scattering, as an option in LAMMPS

code.[7,8] Such a hybrid potential has been widely used in ion bombardment modeling.

As the first step, two graphene planes (160 000 atoms in total) were separated at a distance of 4 nm. The periodical boundary condition was applied. The system was relaxed at 300 K for 10 ps under NVT ensemble with a time step of 0.0025 ps. Then, the system was switched to NVE ensemble with a new time step of 0.0002 ps, and C_{60} molecules bombarded through both graphene layers along the normal direction, at an energy of 250 keV. After deleting the sputtered C atoms, the irradiated system was relaxed for 10 ps under the NVT ensemble with a time step of 0.0025 ps. Next, the top irradiated graphene layer was slowly moved, at an initial speed of 1.5 Å/ps, toward the bottom layer under NVT ensemble. This step was used to simulate layer interactions when they were brought closer during manufacturing. The almost ignorable kinetic energy was absorbed by the system upon soft touching, and van der Walls forces quickly dominated the interaction. The bi-layer was quickly stabilized at a distance of about 0.4 nm, which agrees with the equilibrium plane separation distance in graphite.[9] After two layers touched, structural relaxation and self-alignment, if there were any, were allowed as a function of time (up to 200 ps). The time step was reduced to 0.001 ps. In a parallel study to model gliding of the top graphene layer on the bottom one, a force was applied to create a constant gliding velocity of 0.5 Å/ps under NVT ensemble. The gliding was used to evaluate the friction resistance with or without defect pinning.

Figure 1(a) shows MD simulations of the re-alignment process of pristine graphene, in which the top graphene layer slowly moves toward the bottom one. At the time t = 0, the two graphene layers are intentionally twisted at 1.1°, but at a separation distance of 4 nm. The misalignment creates a periodic moiré pattern as viewed from the top. With a decreasing distance between the two layers, the periodic patterns remain the same. Two layers begin to "touch" each other at time t = 25 ps, corresponding to a separation distance of about 0.4 nm. At time t = 50 ps, the moiré pattern disappears due to self-alignment during the relaxation. Such an automatic alignment is a technological bottleneck for device fabrication requiring high throughput and high repeatability. In comparison, Fig. 1(b) shows top and side views of periodic pattern evolution when two irradiated graphene layers become closer. Both layers are irradiated by three C_{60} clusters prior to the movement. When two layers touch to become a two-layer system,

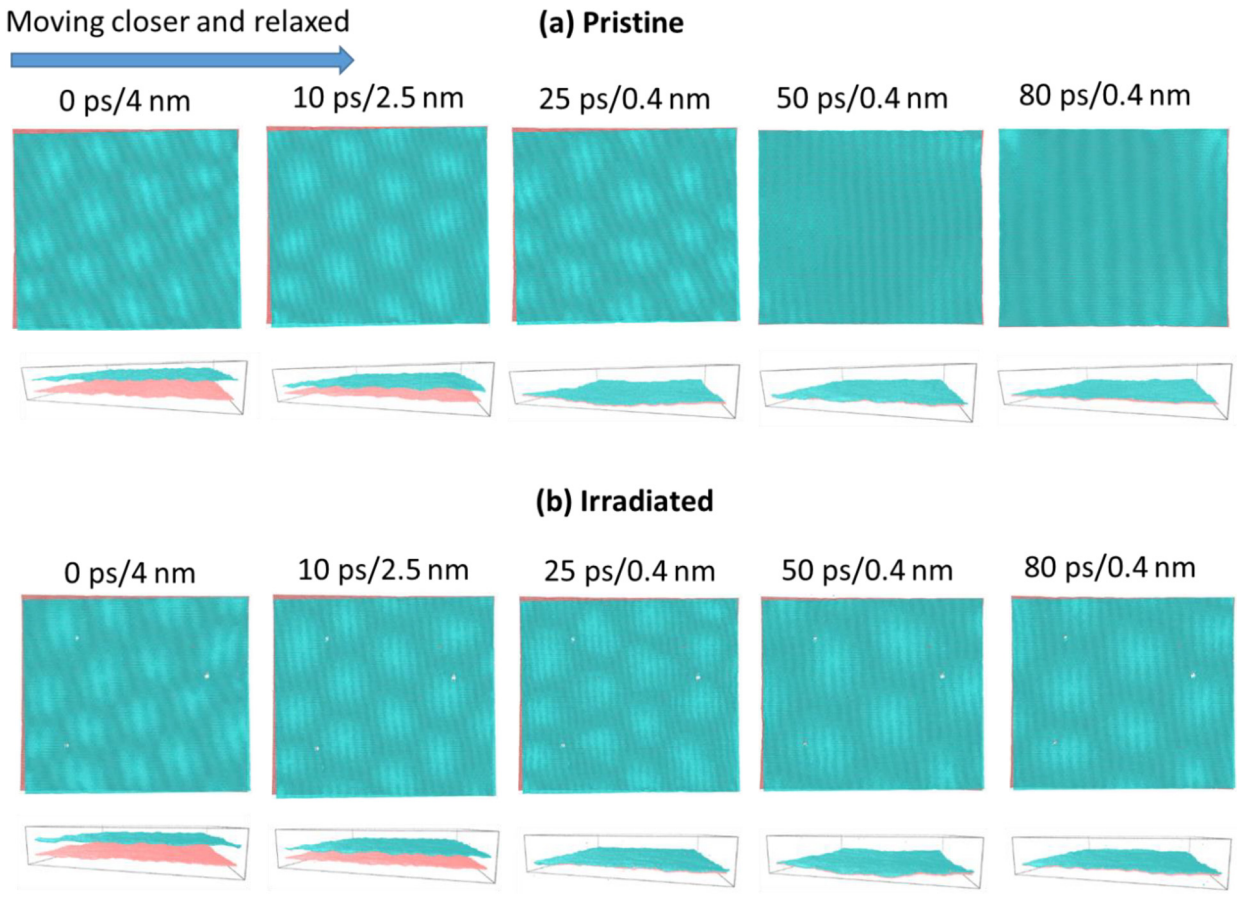

FIG. 1. (a) MD simulations of the top view and side view of two graphene layers moving closer to each other as a function of time and separation distance. The periodic patterns disappear when the two layers touch. (b) Simulations of two irradiated graphene layers moving closer to each other. Prior to movement, the two layers were bombarded with three 250 keV C_{60} clusters.

there is no significant change in the periodic patterns, which suggests a pinning effect.

Figure 2 summarizes the twisting angle changes as a function of time for the pristine system and the irradiated system. The twisting angle is the averaged angle difference between two graphene layers. Fluctuation exists for both systems, even at 300 K. Hence, the local twisting angles vary at different locations, and the error bars represent the fluctuations. The fluctuation is largely caused by plane vibration. Figure 2 shows that the pristine system has reduced twisting angles at a longer time. In contrast, the irradiated system maintains the original twisting angle.

To explain the pinning effect, we show the defect creation in Fig. 3. Figure 3(a) corresponds to the time prior to molecule bombardment, and Fig. 3(b) corresponds to the moment when three molecules pass through the bilayer system. Sputtering and forward knocking on both graphene layers are noticeable. As shown in Fig. 3(c), three molecules hit three points at a triangle configuration. Figures 3(d)–3(f) show the time evolution of the top views of one nanopore created by one molecule, featured by complete removal of atoms in the center and C dangling bonds at the edge.

The major reason for selecting C_{60} molecules as projectiles is that nanopore creation is guaranteed. Molecule–solid interaction is very different from "traditional" ion-solid interactions. For traditional monomer ion bombardment, the cross section (at about 1×10^{-3} Å^2) of displacement creation is significantly less than the size of a target atom (~Å^2). Hence, the damage creation is determined by chance (which means not all ions will create damage). A C_{60} molecule, however, has a size (~7 Å), which is larger than an atom. Therefore, its damage creation (for creating a nanopore) cannot be smaller than the C_{60} cage size. Its pore creation is deterministic (one C_{60} molecule will never miss creating a pore). The nanopore creation is related to the molecule energies. The pore size is maximized when nuclear stopping power of C_{60} molecules reaches its peak value. This corresponds to about 120 keV per molecule, or equivalently 2 keV per carbon atom.

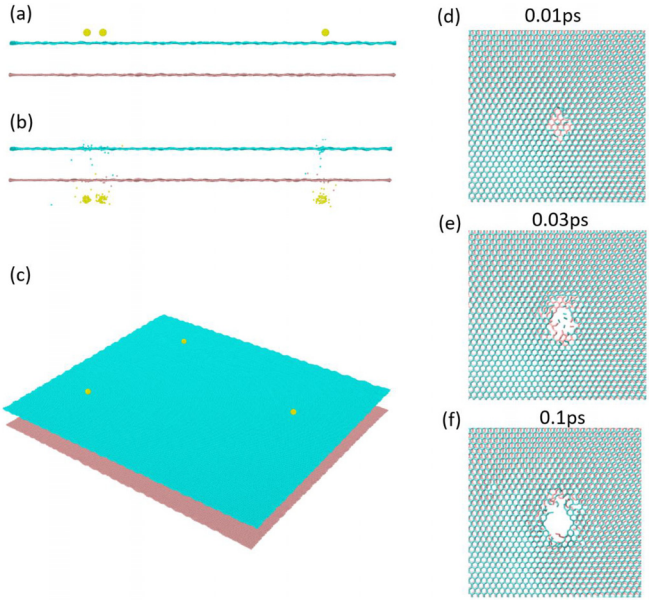

FIG. 3. (a) MD simulations of three 250 keV C_{60} molecules bombarding two graphene layers, which are separated by 4 nm. (b) Sputtering and displacement creations after molecules pass both layers. (c) Top view of irradiated graphene layers. (d)–(f) The nanopore creation and its time evolution.

At lower (<120 keV) or higher energies (>120 keV), the pore size is gradually reduced but cannot be smaller than the molecule size.

Our modeling revealed the atomic-scale details of the defect pinning effect. As shown in Fig. 4, when the two irradiated-graphene layers approach each other, the dangling bonds resulting from C_{60} cluster ion bombardment begin to re-bond upon touching, as highlighted by red circles. The short sp bond is very strong to hold the

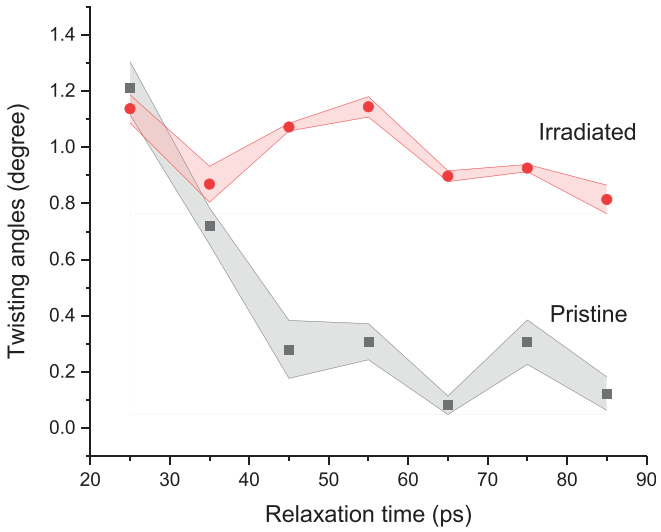

FIG. 2. Twisting angle changes as a function of relaxation time for bi-layer systems with or without C_{60} molecule bombardment. For the irradiated system, the two layers were bombarded with three 250 keV C_{60} molecules.

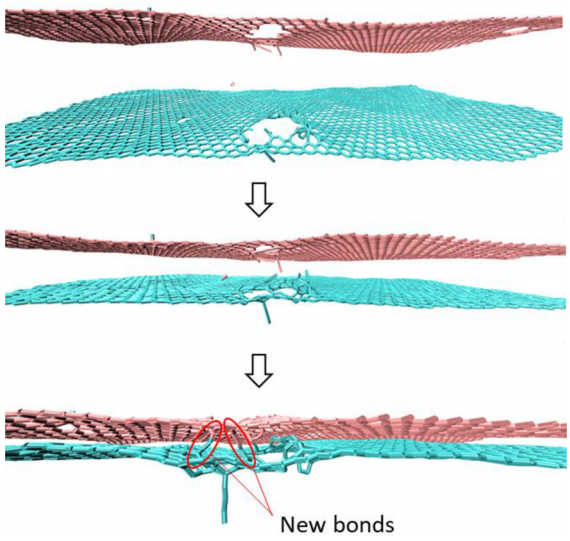

FIG. 4. Interactions of two approaching graphene layers. Both layers are pre-irradiated with 3 C_{60} molecules.

systems. The effect becomes obvious when the top layer is intentionally moved under a forced sliding. Figure 5(a) shows the gliding of two layers under shear stress for the testing of bonding strength. The displacement results in the formation of one-dimensional long carbon chains, which can be as long as >10 nm. Such chain formation makes debonding and gliding difficult. Therefore, the immobilized structures are stable upon thermal vibration and small shear force loading.

The chain formation process involves both pulling atoms from the pore edge and reconstructions of the rest of the atoms around the edge. Figure 5(b) shows the schematics of the chain formation observed. The last atom (marked as "1") at the chain end often has a bonding with two edge atoms (marked as atoms "2" and "3"). Each edge atom forms σ-bonds with neighbors. Then one of the edge atoms (atom "2") breaks σ-bonding, becomes a new chain end, and forms new σ-bonds with two different edge atoms ("3" and "4"). The process repeats, and atom "3" becomes the next chain end. All chain atoms, except for the chain end, form an sp bond with their chain neighbors.

Figure 5(c) shows the potential changes in the system as a function of time or, equivalently, horizontal displacement. Only one localized area containing one nanopore is used for the analysis. The analysis area does not include the whole graphene plane since the graphene edge, once moving out of the two-layers' overlapping area, will lead to a potential increase. As shown in Fig. 5(c), the molecule-irradiated system shows a quick potential increase, arising from the friction force contributed by a single C chain formation. In comparison, graphene sliding is almost friction-free for the pristine system.

Single chain as long as >10 nm is observed. The chain breaking is not caused by too much bond stretching. With increasing chain length, the chain becomes more and more parallel to the graphene plane. When the chain is too close to one graphene atom, it intends to form either sp^2 or sp^3 bonds and breaks the original sp bond along the chain. The maximum chain length is sensitive to temperature. Large thermal vibration of graphene at a high temperature will increase the interaction of the chain atoms with other graphene atoms, hence facilitating the chain breaking.

The formation of a one-dimensional carbon chain has been predicted by modeling and experimentally observed in many carbon systems under various conditions.[10–24] For example, single chains were experimentally created by gas-phase deposition, epitaxial growth, electrochemical synthesis, electron irradiation of carbon nanoribbons, and coalescence of fullerenes.[10–19] Single chains were also predicted by modeling in sliding of graphene/SiC composite, edge interactions of graphene islands, and twisting of carbon nanotube bundles.[20–24]

Theoretically, using defective zones to immobilize graphene rotation and sliding does not necessarily require molecule bombardment or ion bombardment. If one carbon interstitial is trapped between two graphene layers, the individual carbon atoms can induce chain formation upon graphene gliding. Such interstitial induced chain formation is most effective when a vacancy is nearby since two dangling bonds intend to interact easily with an energy barrier lower than the case having one dangling bond and one C lattice atom in a perfect sixfold ring. This further suggests that natural defects without irradiation may induce chain formation, but at much lower efficiency.

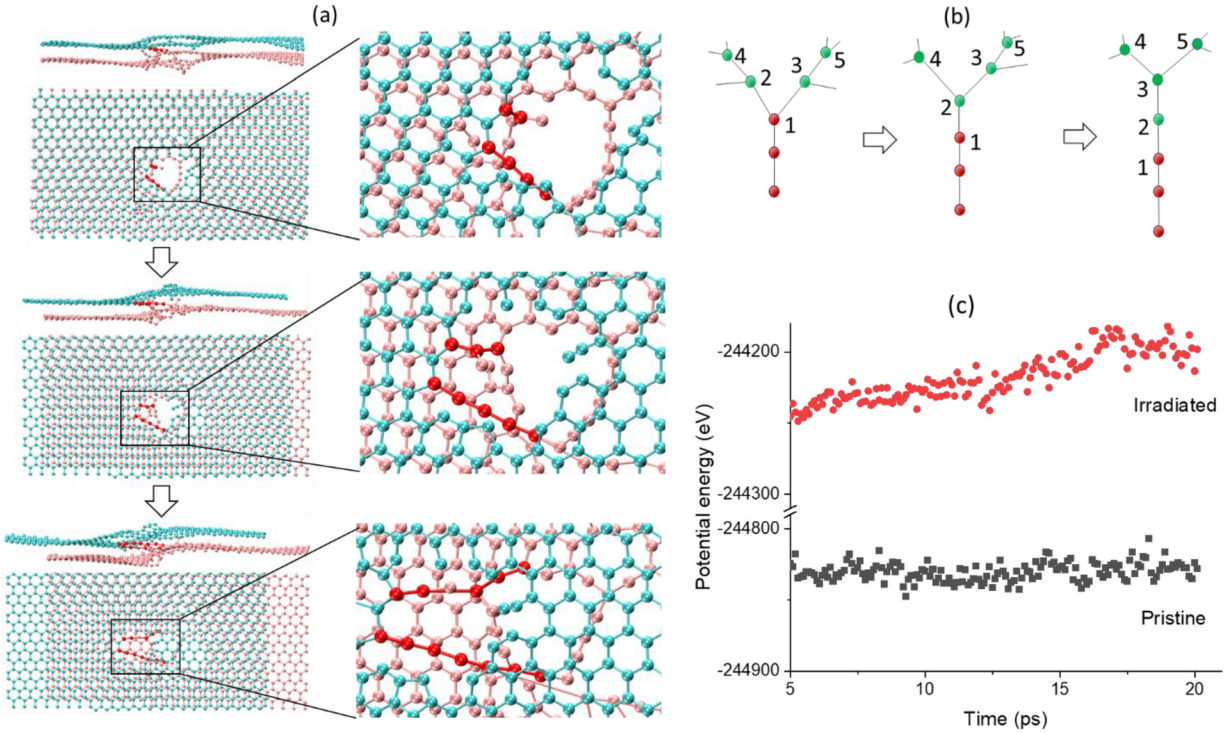

FIG. 5. (a) The side and top views of irradiated bi-layer graphene upon sliding. (b) Schematics of the carbon chain formation. (c) Potential energy changes of bi-layer graphene upon sliding, as a function of time, for the case with or without molecule bombardment.

There is no evidence that nanopores on graphene will be self-healed automatically. High-resolution images of sub-nanometer pores on graphene were obtained from numerous studies.[25,26] Imaging pores using transmission electron microscopy was challenging and problematic due to electron-beam assisted "epitaxial growth," in which a pore can be filled with hydrocarbon from contaminations.[25,27] Such healing can be avoided, however, through careful control of electron beam voltage, vacuum level, and cleanliness of graphene.[25,28] For example, high-temperature annealing prior to imaging can prevent pore filling.[25,28]

MD simulations did not include electronic stopping. However, the effect is believed to be ignorable in the present study based on the following reasons: (1) For our selected C_{60} molecule bombardment at equivalent energy of ~4.2 keV per carbon atom, the ratio of electronic stopping to nuclear stopping is about 0.6 by ignoring the unknown molecule effect. The amount of energy deposition from the electron stopping is very small, considering that the substrate is only a monolayer; (2) previous studies on low energy (20–30 keV) C ion bombardment in bulk SiC show an almost ignorable difference in total numbers of defects created and a small effect on defect size distributions.[29] For graphene, which has a superior thermal conductivity, the electron heating effect should be weak, if not weaker; (3) By repeating the same molecule bombardment at two different temperatures (300 K vs 500 K), our comparison studies show similar pore structures. This suggests that substrate temperature effects are not significant even under such an exaggerated condition.

The simulations move the top graphene plane at an initial speed of 1.5 Å/ps to slowly approach the bottom graphene plane. Note that the plane rotation occurs during the subsequent structural relaxation at a much later time (>20 ps), instead of the movement prior to touching. Hence, the layer rotation is not influenced by the details of the touching setup. The speed of 1.5 Å/ps is close to the final approaching speed of two layers that freely approach each other under van der Waals interactions. For an initial separation distance of 1 nm, it takes about 8 ps to touch two layers which are static at the beginning. Prior to the final touching, the speed reaches about 2 Å/ps. For a larger initial separation distance of 2 nm, it takes a much longer time to slowly move to a distance ~1 nm, following by the same fast approaching as the 1 nm separation distance. No plane rotation occurs during the approaching stage, for both initial separation distances of 1 nm and 2 nm.

The present study is limited to the modeling only since it is challenging for us, at the current stage, to demonstrate the feasibility experimentally. But the concept here provides guidance for future experiments. Note that direct observation of Moiré fringe is not trivial. Several techniques were recently developed to characterize graphene bilayers or similar structures. These methods include combined near-field IR microscopy and scanning probe microscopy,[30] ultra-low energy transmission electron microscopy,[31] ultra-low voltage aberration-corrected scanning tunneling microscopy,[32] and high vacuum scanning tunneling microscopy.[33]

In summary, we propose a method to fabricate bi-layer graphene of a specific twisting angle, with high throughput and high repeatability. Automatic alignment during the relaxation of two touching layers makes the process challenging and almost uncontrollable. We demonstrate the feasibility of pinning two layers of graphene by using irradiation-induced defects. The method includes the step of using C_{60} molecule bombardment to create nanopores on both graphene layers and the step of allowing two layers close to each other to bond into a bi-layer system. The dangling bonds of the defective zones on each layer interact with each other to re-bond, which is strong enough to immobilize graphene rotation and automatic alignment. The modeling shows that relative movement between two layers will induce carbon single-chain defects, resulting in strong friction forces.

This work was supported by the U.S. Department of Energy, Office of Basic Energy Sciences, under Grant No. DE-SC0006725. The High-Performance Research Computing (HPRC) center at Texas A&M University provided the computational resources required for this work.

DATA AVAILABILITY

The data that support the findings of this study are available from the corresponding author upon reasonable request.

REFERENCES

[1]Y. Cao, V. Fatemi, A. Demir, S. Fang, S. L. Tomarken, J. Y. Luo, J. D. Sanchez-Yamagishi, K. Watanabe, T. Taniguchi, E. Kaxiras, R. C. Ashoori, and P. Jarillo-Herrero, "Correlated insulator behaviour at half-filling in magic-angle graphene superlattices," Nature **556**, 80–84 (2018).
[2]Y. Cao, V. Fatemi, S. Fang, K. Watanabe, T. Taniguchi, E. Kaxiras, and P. Jarillo-Herrero, "Unconventional superconductivity in magic-angle graphene superlattices," Nature **556**, 43–50 (2018).
[3]E. Gibney, "Superconductivity with a twist," Nature **565**, 15–18 (2019).
[4]S. Plimpton, "Fast parallel algorithms for short-range molecular dynamics," J. Comput. Phys. **117**, 1–19 (1995).
[5]S. J. Stuart, A. B. Tutein, and J. A. Harrison, "A reactive potential for hydrocarbons with intermolecular interactions," J. Chem. Phys. **112**, 6472–6486 (2000).
[6]G. E. Bacon, "The interlayer spacing of graphite," Acta Crystallogr. **4**, 558–561 (1951).
[7]J. Tersoff, "Modeling solid-state chemistry: Interatomic potentials for multicomponent systems," Phys. Rev. B **39**, 5566–5568 (1989).
[8]J. F. Ziegler, J. P. Biersack, and U. Littmark, *Stopping and Ranges of Ions in Matter* (Pergamon Press, Oxford, 1985).
[9]O. Hod, "Graphite and hexagonal boron-nitride have the same interlayer distance. Why?," J. Chem. Theory Comput. **8**, 1360–1369 (2012).
[10]I. E. Castelli, P. Salvestrini, and N. Manini, "Mechanical properties of carbynes investigated by *ab initio* total-energy calculations," Phys. Rev. B **85**, 214110 (2012).
[11]Z. Zanolli, G. Onida, and J. C. Charlier, "Quantum spin transport in carbon chains," ACS Nano **4**, 5174–5180 (2010).
[12]N. Lang and P. Avouris, "Electrical conductance of parallel atomic wires," Phys. Rev. B **62**, 7325–7329 (2000).
[13]R. J. Lagow, J. J. Kampa, H. C. Wei, S. L. Battle, J. W. Genge, D. A. Laude, C. J. Harper, R. Bau, R. C. Stevens, J. F. Haw, and E. Munson, "Synthesis of linear acetylenic carbon: The '*sp*' carbon allotrope," Science **267**, 362–367 (1995).
[14]L. Kavan, J. Hlavatý, J. Kastner, and H. Kuzmany, "Electrochemical carbyne from perfluorinated hydrocarbons: Synthesis and stability studied by Raman scattering," Carbon **33**, 1321–1329 (1995).
[15]C. S. Casari, A. L. Bassi, L. Ravagnan, F. Siviero, C. Lenardi, P. Piseri, G. Bongiorno, C. E. Bottani, and P. Milani, "Chemical and thermal stability of carbyne-like structures in cluster-assembled carbon films," Phys. Rev. B **69**, 075422 (2004).
[16]F. Cataldo, "Polyynes: Synthesis," in *Properties, and Applications* (CRC Press, Boca Raton, 2005).
[17]C. Jin, H. Lan, L. Peng, K. Suenaga, and S. Iijima, "Deriving carbon atomic chains from graphene," Phys. Rev. Lett. **102**, 205501 (2009).
[18]E. Hobi, R. B. Pontes, A. Fazzio, and A. J. R. da Silva, "Formation of atomic carbon chains from graphene nanoribbons," Phys. Rev. B **81**, 201406 (2010).

[19]A. Chuvilin, J. C. Meyer, G. Algara-Siller, and U. Kaiser, "From graphene constrictions to single carbon chains," New J. Phys. **11**, 083019 (2009).
[20]F. Börrnert, C. Börrnert, S. Gorantla, X. Liu, A. Bachmatiuk, J. O. Joswig, F. R. Wagner, F. Schäffel, J. H. Warner, R. Schönfelder, B. Rellinghaus, T. Gemming, J. Thomas, M. Knupfer, B. Büchner, and M. H. Rümmeli, "Single-wall-carbon-nanotube/single-carbon-chain molecular junctions," Phys. Rev B **81**, 085439 (2010).
[21]I. E. Castelli, N. Ferri, G. Onida, and N. Manini, "Carbon sp Chains in Graphene Nanoholes," J. Phys.: Condens. Matter **24**, 104019 (2012).
[22]C. Ataca and S. Ciraci, "Perpendicular growth of carbon chains on graphene from first-principles," Phys. Rev. B **83**, 235417 (2011).
[23]Y. Wang, Z. Z. Lin, W. Zhang, J. Zhuang, and X. J. Ning, "Pulling long linear atomic chains from graphene: Molecular dynamics simulations," Phys. Rev. B **80**, 233403 (2009).
[24]J. B. Wallace, D. Chen, and L. Shao, "Carbon displacement induced single carbon atomic chain formation and its effects on sliding of SiC fibers in SiC/graphene/SiC composite," Mater. Res. Lett. **4**, 55–61 (2016).
[25]A. W. Robertson, G.-D. Lee, K. He, C. Gong, Q. Chen, E. Yoon, A. I. Kirkland, and J. H. Warner, "Atomic structure of graphene subnanometer pores," ACS Nano **9**, 11599–11607 (2015).
[26]T. Yang, H. Lin, X. Zheng, K. P. Loh, and B. Jia, "Tailoring pores in graphene-based materials: From generation to applications," J. Mater. Chem. A. **5**, 16537 (2017).
[27]R. Zan, Q. M. Ramasse, U. Bangert, and K. S. Novoselov, "Graphene reknits its holes," Nano Lett. **12**, 3936–3940 (2012).
[28]A. W. Robertson, C. S. Allen, Y. A. Wu, K. He, J. Olivier, J. Neethling, A. I. Kirkland, and J. H. Warner, "Spatial control of defect creation in graphene at the nanoscale," Nat. Commun. **3**, 1144 (2012).
[29]E. Zarkadoula, G. Samolyuk, Y. Zhang, and W. J. Weber, "Electronic stopping in molecular dynamics simulations of cascades in 3C–SiC," J. Nucl. Mater. **540**, 152371 (2020).
[30]Y. Luo, R. Engelke, M. Mattheakis, M. Tamagnone, S. Carr, K. Watanabe, T. Taniguchi, E. Kaxiras, P. Kim, and W. L. Wilson, "In situ nanoscale imaging of moiré superlattices in twisted van der Waals heterostructures," Nat. Commun. **11**, 4209 (2020).
[31]H. Yoo, R. Engelke, S. Carr, S. Fang, K. Zhang, P. Cazeaux, S. H. Sung, R. Hovden, A. W. Tsen, T. Taniguchi, K. Watanabe, G.-C. Yi, M. Kim, M. Luskin, E. B. Tadmor, E. Kaxiras, and P. Kim, "Atomic and electronic reconstruction at the van der Waals interface in twisted bilayer graphene," Nat. Mater. **18**, 448–453 (2019).
[32]Y. Jiang, Z. Chen, Y. Han, P. Deb, H. Gao, S. Xie, P. Purohit, M. W. Tate, J. Park, S. M. Gruner, V. Elser, and D. A. Muller, "Electron ptychography of 2D materials to deep sub-ångström resolution," Nature **559**, 343–349 (2018).
[33]A. Kerelsky, L. J. McGilly, D. M. Kennes, L. Xian, M. Yankowitz, S. Chen, K. Watanabe, T. Taniguchi, J. Hone, C. Dean, A. Rubio, and A. N. Pasupathy, "Maximized electron interactions at the magic angle in twisted bilayer graphene," Nature **572**, 95–100 (2019).